Available online at www.sciencedirect.com
SCIENCE DIRECT®
Journal of Molecular Spectroscopy 232 (2005) 174–185
Journal of MOLECULAR SPECTROSCOPY
www.elsevier.com/locate/jms

Microwave and high resolution infrared spectra of vinyl chloride, ab initio anharmonic force field and equilibrium structure

J. Demaison [a,*], H. Møllendal [b], A. Perrin [c], J. Orphal [c], F. Kwabia Tchana [c], H.D. Rudolph [d], F. Willaert [a]

[a] Laboratoire de Physique des Lasers, Atomes, et Molécules, UMR CNRS 8523, Université de Lille I, F-59655 Villeneuve d'Ascq Cédex, France
[b] Department of Chemistry, University of Oslo, P.O. Box 1033, Blindern, NO-0315 Oslo, Norway
[c] Laboratoire Interuniversitaire des Systèmes Atmosphériques (LISA), UMR CNRS 7583, 61 av. Charles de Gaulle, F-94010 Créteil Cédex, France
[d] Department of Chemistry, University of Ulm, D-89069 Ulm, Germany

Received 4 March 2005
Available online 23 May 2005

Abstract

The quadratic, cubic, and semi-diagonal quartic force field of vinyl chloride has been calculated at the MP2 level of theory employing a basis set of triple-ζ quality. The spectroscopic constants derived from this force field are compared with the experimental values. To make this comparison more complete, the rotational constants of the lowest excited state, $v_9 = 1$ at 395 cm^{-1} have been determined by microwave spectroscopy and the v_{12} band (around 618 cm^{-1}) has been investigated by high-resolution infrared Fourier transform spectroscopy. The equilibrium structure has been derived from experimental ground state rotational constants and ab initio rovibrational interaction parameters. This semi-experimental structure is in excellent agreement with the ab initio structure calculated at the CCSD(T) level of theory using a basis set of quintuple-ζ quality and a core correlation correction. The experimental mass-dependent r_m structures are also determined and their accuracy is discussed. The recommended equilibrium geometry is: $r(C{=}C) = 1.3262(10)$, $r(C{-}Cl) = 1.7263(10)$, $r(C{-}H_g) = 1.0784(10)$, $r(C{-}H_c) = 1.0795(10)$, $r(C{-}H_t) = 1.0797(10)$, $\angle(CCCl) = 122.77(10)°$, $\angle(CCH_g) = 123.86(10)°$, $\angle(CCH_c) = 121.80(10)°$, $\angle(CCH_t) = 119.29(10)°$.

Keywords: Anharmonic force field; Ab initio; Equilibrium structure; Vinyl chloride; Microwave; Infrared

1. Introduction

The determination of the accurate equilibrium structure of a polyatomic molecule of more than three atoms remains a formidable task. Several methods are indeed available but, although they are known to give good results for triatomic molecules, reliable results for larger molecules are still scarce [1]. We have undertaken a systematic comparison of the experimental mass-dependent (r_m) structure [2] with the ab initio structure and the semi-experimental structure (obtained from the experimental ground state constants corrected with the ab initio rotation–vibration interaction constants) [3]. The goal is to check the accuracy of the r_m structures and to determine the factors which may affect it as well as to detect possible shortcomings in the ab initio and semi-experimental methods. We report here the results for the hexaatomic molecule vinyl chloride, $H_2C{=}CHCl$.

Vinyl chloride is a major industrial product used mainly for PVC production. Smaller amounts of vinyl chloride are used in furniture and automobile upholstery. In the atmosphere, it reacts with hydroxyl radicals and ozone, ultimately forming formaldehyde, carbon monoxide, hydrochloric acid, and formic acid. It is considered to be a carrier for chlorine transported into the troposphere and stratosphere and it is a potential threat for ozone depletion. Its average internuclear distances

* Corresponding author. Fax: +33 3 20 33 70 20.
E-mail address: jean.demaison@univ-lille1.fr (J. Demaison).

0022-2852/$ - see front matter © 2005 Elsevier Inc. All rights reserved.
doi:10.1016/j.jms.2005.04.006

(r_g) have been obtained in 1972 by gas-phase electron diffraction [4]. There are also several determinations of the substitution (r_s) structure by microwave spectroscopy [5,6]. In the latter work, the rotational constants of 20 isotopologs are given. However, the *b*-coordinates of the chlorine and H_{trans} atoms are so small that the solutions of the Kraitchman equations are not reliable. Recently, the r_m^ρ structure has been calculated and the millimeterwave and submillimeterwave spectra of the main isotopic species have been analyzed permitting an accurate determination of the centrifugal distortion constants [7]. The ab initio structure has also been calculated many times. Particularly, Coffey et al. [8] calculated an ab initio structure which was empirically corrected to obtain r_0 values. They found a good agreement with the experimental r_0 structure. However, the r_0 structure is purely empirical and is often significantly different from the equilibrium (r_e) structure. Merke et al. [7] calculated a new ab initio structure employing the second-order Møller–Plesset perturbation theory (MP2) [9] and a near-equilibrium structure was estimated using offsets derived empirically. This structure was found to be in good agreement with the r_m^ρ structure.

Low resolution infrared spectra were recorded a long time ago [10–12] and all fundamental vibrations as well as some combination bands were assigned. The medium-resolution spectra of some bands were analyzed taking into account the Coriolis interactions [13]. De Lorenzi and co-workers have analyzed the high resolution infrared spectra of the lowest fundamental bands ν_5 [14], ν_6 [15,16], ν_7 [17], ν_8 [18], and ν_{10} and ν_{11} [19]. To check the quality of the ab initio anharmonic force field which will be used to calculate the semi-experimental structure, it is useful to have the experimental band centers, the ground state sextic centrifugal distortion constants and the rotation–vibration interactions constants (α-constants). However, the parameters of two low-lying vibrational states $\nu_9 = 1$ at 395 cm^{-1} and $\nu_{12} = 1$ at 618 cm^{-1} are still missing.

In the first part of this paper, the analysis of the microwave spectrum of the $\nu_9 = 1$ state is reported. In the second part, the high resolution infrared spectrum of the ν_{12} band is described. In the third part, the ab initio structure is calculated. In the fourth part, the ab initio anharmonic force field is given, the ab initio and experimental molecular parameters are compared and the semi-experimental equilibrium structure is deduced. Finally, in the last part, the empirical r_m structures are calculated and the different structures are compared.

2. Microwave spectrum of the $\nu_9 = 1$ state

The rotational spectrum was studied using the Oslo Stark spectrometer which is described briefly in [20]. The accuracy of the spectral measurements is about 0.1 MHz for isolated lines but some lines are overlapped by much stronger ground state lines.

A first approximate prediction of the spectrum was made using the ab initio α-constants (see Section 5, below) and the ground state nuclear quadrupole coupling constants [21]. The *a*-type lines were rather readily assigned but only one *b*-type could be tentatively assigned. It was not included in the final fit. The experimental frequencies are given in Table 1. The quadrupole coupling constants were calculated using the splittings of the three $J = 2 \leftarrow 1$ transitions. Their values (in MHz), $\chi_{bb} + \chi_{cc} = 57.90(16)$ and $\chi_{bb} - \chi_{cc} = -6.72(37)$ are close to the corresponding values of the ground state (57.21(20) and −6.27(24), respectively [6,21]). The experimental frequencies were corrected for the quadrupole hyperfine structure using these constants and the hypothetical unsplit frequencies were fitted using a Watson–Hamiltonian in the *A*-reduction and I^r representation. Most of the centrifugal distortion constants were fixed to the ground state values [7]. The derived parameters are given in Table 1. If the *b*-type line is included in the fit, it gives $A = 57053.7(8)$ MHz. The derived inertial defect, $\Delta_9 = 0.2358$ u Å^2 is in perfect agreement with the value calculated from the harmonic force field (see Section 5 and Table 11).

Table 1
Experimental frequencies (MHz) and molecular parameters for the $\nu_9 = 1$ state of $H_2C{=}CH^{35}Cl$

J'	K'_a	K'_c	J''	K''_a	K''_c	Exp.	e − c
2	0	2	1	0	1	22925.02	0.10
2	1	2	1	1	1	22340.32	−0.18
2	1	1	1	1	0	23520.11	0.28
3	0	3	2	0	2	34374.23	−0.05
3	1	3	2	1	2	33507.04	−0.17
4	1	4	3	1	3	44670.02	0.30
4	1	3	3	1	2	47027.82	−0.23
5	0	5	4	0	4	57220.81	0.10
5	1	5	4	1	4	55826.57	−0.13
5	3	3	4	3	2	57343.37	0.29
5	1	4	4	1	3	58775.98	1.90
5	3	2	4	3	1	57343.37	−0.28
6	0	6	5	1	5	21566.17	0.00

Molecular parameters (unit)	Value[a]
B[b](MHz)	6027.4308(45)
C (MHz)	5437.6751(44)
Δ_J[c] (Hz)	6.69(80)
Δ_{JK} (kHz)	−41.3(31)
Standard deviation (kHz)	147

[a] Errors given in parentheses are in unit of the last digit.
[b] If the *b*-type line is included in the fit, $A = 57053.7(8)$ MHz.
[c] The other centrifugal distortion constants are fixed at the ground state values [7].

3. Fourier transform spectrum of the ν_{12} band

3.1. Experimental details

The high-resolution (0.004 cm^{-1} unapodized resolution) room-temperature absorption spectra of vinyl chloride were recorded using the Bruker IFS 120 HR Fourier transform spectrometer (FTS) located at LISA. The spectrometer was set up with a Mylar/Germanium "compound" beamsplitter, He-cooled Si = 20 bolometer, and optical and electronic filters to obtain a useful bandpass of 450–670 cm^{-1}. A Globar source was used. The sample of CH_2=CHCl in natural abundance (Fluka, >99.5% stated purity) was introduced at a $P = 9.1$ mbar pressure (MKS Baratron 10 mbar head) in a 25 cm long Pyrex cell with CsBr windows.

Line centers were determined from the absorption spectra using the peakfinder routine in the Bruker OPUS software. The absolute wavenumber calibration was performed using 10 residual H_2O lines together with the IUPAP recommended line positions of [22]. The accuracy of the wavenumber calibration is about 0.0003 cm^{-1} (root-mean-square).

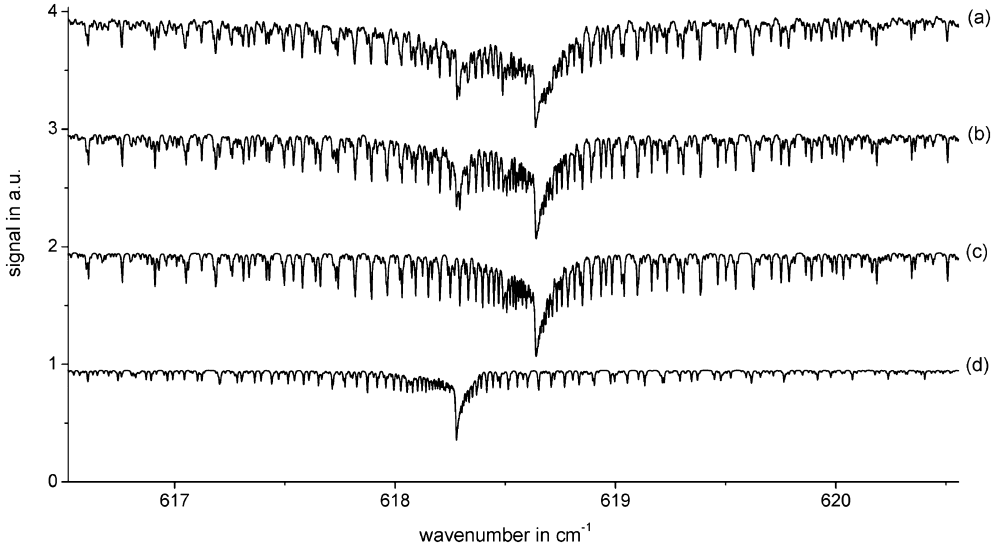

Fig. 1. The central part of the ν_{12} bands of vinyl chloride. The agreement between the observed spectrum (trace a) and the calculated one (trace b) is excellent, proving the quality of the calculation. Traces c and d give the detailed calculated contribution for the CH_2=$CH^{35}Cl$ and CH_2=$CH^{37}Cl$ species, respectively.

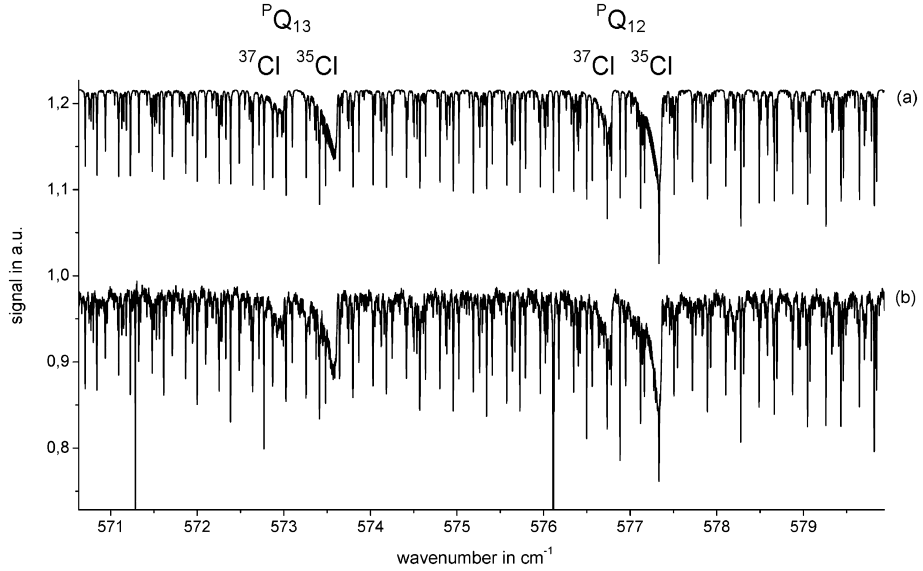

Fig. 2. Portion of the P branch of the ν_{12} band of vinyl chloride. Calculated spectrum (trace a) and observed spectrum (trace b). In this spectral region, examples of regular series of ${}^{P}Q_{K_a}$ structures are observable near 573.6 and 577.4 cm^{-1} for $K''_a = 13$ and $K''_a = 12$, respectively.

3.2. Analysis

The ν_{12} band is a pure C-type band for symmetry reasons. As can be seen on Figs. 1 and 2 the spectrum of this prolate asymmetric rotor ($A \sim 1.90$, $B \sim 0.200$, and $C \sim 0.182\ \mathrm{cm}^{-1}$) is rather congested owing to comparatively small values of the B and C rotational constants and of the presence of lines from both the $CH_2{=}CH^{35}Cl$ and $CH_2{=}CH^{37}Cl$ isotopologs. Fortunately it was possible to take advantage of some regularities in the spectrum. For example for the high K_a values, the ${}^{P}Q_{K_a}$ and ${}^{R}Q_{K_a}$ subbranches are structured in stacks of lines separated by about $(A-(B{+}C)/2)$ grouping together transitions with the same K_a quantum number. On the other hand, the central parts of the $CH_2{=}CH^{35}Cl$ and $CH_2{=}CH^{37}Cl$ Q-branches are rather congested. The analyses of the ν_{12} bands of $CH_2{=}CH^{35}Cl$ and $CH_2{=}CH^{37}Cl$ were started taking advantage of the regularities described above. After a few lines had been assigned, the accurate ground-state spectroscopic constants in the Watson A-reduction I^r-representation taken from [7] were used to get a first set of the upper-state spectroscopic constants. With these first constants, it was possible to make better predictions and to assign new lines. The process was repeated until it was no longer possible to obtain new assignments. Table 2 gives the ranges of assigned energy levels for the $CH_2{=}CH^{35}Cl$ and $CH_2{=}CH^{37}Cl$ species.

3.3. Energy level calculations

Using the improved sets of ground state constants which were obtained recently [7] for $CH_2{=}CH^{35}Cl$ and $CH_2{=}CH^{37}Cl$ the experimental energy levels of the 12^1 upper vibrational state analyzed in this work were computed by adding the corresponding $CH_2{=}CH^{35}Cl$ and $CH_2{=}CH^{37}Cl$ ground-state energies to the observed line positions.

The infrared energy levels for 12^1 state were least-squares fitted assuming that there are no interactions perturbing the 12^1 levels. Using a Watson A-type Hamiltonian written in I^r representation, it was possible to get a first set of 12^1 upper state constants. However, such a model proved not to be fully satisfactory. Actually, the number of flexible parameters to be used to reproduce the 12^1 energy levels within their experimental uncertainty was rather important. In fact all quartic centrifugal distortion constants together with the Φ_K parameters had to be adjusted. According to the ab initio predictions this is due to the existence of a weak but significant A-type Coriolis interaction linking the 12^1 and 8^1 levels. This was confirmed when examining in detail the study performed for the ν_8 band of vinyl chloride in [18]. At that time no data were available at high resolution for the 12^1 state, and consequently the 8^1 energy levels calculation was performed neglecting the $8^1 \iff 12^1$ resonance. Therefore, a rather large set of flexible parameters had to be adjusted for 8^1 (the Φ_J, Φ_{KJ}, Φ_K, and ϕ_J together with the band center, the rotational constants, and all quartic centrifugal distortion constants).

Table 2
Results of the assignments for the ν_{12} band

	No. of lines	No. of levels	J range	K_a range
$CH_2CH^{35}Cl$	1563	1100	2–53	0–17
$CH_2CH^{37}Cl$	658	475	1–44	0–14

It was therefore decided to take the A-type Coriolis interaction linking the 12^1 and 8^1 levels into account, taking advantage of the fact that a list of experimental energy levels is now available both for the 12^1 and 8^1 vibrational states. Accordingly, the experimental energy levels of the 8^1 upper vibrational state were computed for $CH_2{=}CH^{35}Cl$ and $CH_2{=}CH^{37}Cl$ from the list of assigned ν_8 transitions given in [18]. The final calculation of the $\{12^1, 8^1\}$ resonating energy levels was performed using the Hamiltonian model given in Table 3. The v-diagonal part of the Hamiltonian model consists of the A-reduced Watson type Hamiltonians written in the I^r representation, while the off diagonal operators are A-type Coriolis operators. The Hamiltonian constants resulting from the final least-squares fit are given together with their estimated uncertainties in Tables 4 and 5 for the $CH_2{=}CH^{35}Cl$ and $CH_2{=}CH^{37}Cl$ isotopic species, respectively. In this fit, the higher order centrifugal distortion constants for the 12^1 and 8^1 states were fixed at their ground state values [7].

It is gratifying to observe that the value derived from the least-squares fit for the first order A-type Coriolis operator parameter ${}^{\mathrm{EXP}}C_A^1$ is in good agreement with the value predicted by the present ab initio calculations (see below). Actually, from the equation

Table 3
Hamiltonian model used for the $\{12^1, 8^1\}$ resonating states of $CH_2{=}CH^{35}Cl$ and $CH_2{=}CH^{37}Cl$

	$\{v, v'\}=\{12^1, 8^1\}$	
	$\mathbf{v}$	$\mathbf{v}'$
$\mathbf{v}$	H_W	Herm. conj.
$\mathbf{v}'$	$\mathbf{C}_A$	H_W

$$\begin{aligned}\mathbf{H}_W = {} & E_v + [A^v - 1/2(B^v + C^v)]\mathbf{J}_z^2 + 1/2(B^v + C^v)\mathbf{J}^2 \\ & + 1/2(B^v - C^v)\mathbf{J}_{xy}^2 - \Delta_K^v \mathbf{J}_z^4 - \Delta_{JK}^v \mathbf{J}_z^2 \mathbf{J}^2 - \Delta_J^v (\mathbf{J}^2)^2 \\ & - \delta_K^v \{\mathbf{J}_z^2, \mathbf{J}_{xy}^2\} - 2\delta_J^v \mathbf{J}_{xy}^2 \mathbf{J}^2 + \Phi_K^v \mathbf{J}_z^6 + \Phi_{KJ}^v \mathbf{J}_z^4 \mathbf{J}^2 \\ & + \Phi_{JK}^v \mathbf{J}_z^2 (\mathbf{J}^2)^2 + \Phi_J^v (\mathbf{J}^2)^3 + \phi_K^v \{\mathbf{J}_z^4, \mathbf{J}_{xy}^2\} \\ & + \phi_{KJ}^v \{\mathbf{J}_z^2, \mathbf{J}_{xy}^2\} \mathbf{J}^2 + 2\phi_J^v \mathbf{J}_{xy}^2 (\mathbf{J}^2)^2 + \cdots\end{aligned}$$

$$\mathbf{C}_A = C_A^1 \mathbf{J}_z + C_A^2 \{\mathrm{i}\mathbf{J}_y, \mathbf{J}_x\} \cdots$$

Table 4
Hamiltonian constants for the $\{12^1,8^1\}$ resonating states of $CH_2{=}CH^{35}Cl$

	12^{1a}	8^1
E_v (cm^{-1})	618.57314(16)	720.92104(11)
A (MHz)	57007.95(130)	56738.77(130)
B (MHz)	6024.9946(300)	5999.44531(720)
C (MHz)	5447.4385(310)	5419.37012(590)
Δ_J (kHz)	[b]	3.070871(690)
Δ_{JK} (kHz)	[b]	[b]
Δ_K (kHz)	[b]	1374.957(430)
δ_J (kHz)	[b]	0.443954(660)
δ_K (kHz)	[b]	[b]
Φ_J	[b]	[b]
Φ_{JK}	[b]	[b]
Φ_{KJ}	[b]	[b]
Φ_K	[b]	[b]
ϕ_K	[b]	[b]
ϕ_{JK}	[b]	[b]
ϕ_J	[b]	[b]
Interacting constant (in MHz): $C_A^1 = 47857.0(400)$		

[a] When the Coriolis interaction is neglected (in MHz): $A = 56261.88(13)$, $B = 6024.762(57)$, $C = 5447.768(61)$.
[b] Fixed at the ground-state value [7].

Table 5
Hamiltonian constants for the $\{12^1,8^1\}$ resonating states of $CH_2{=}CH^{37}Cl$

	12^{1a}	8^1
E_v (cm^{-1})	618.21940(24)	715.40824(13)
A (MHz)	56913.95(150)	56664.26(150)
B (MHz)	5898.5459(640)	5873.7666(150)
C (MHz)	5343.5415(670)	5315.9458(120)
Δ_J (kHz)	2.9492(120)	2.948237(860)
Δ_{JK} (kHz)	[b]	−41.8657(550)
Δ_K (kHz)	1227.73(130)	1372.374(520)
δ_J (kHz)	0.3526(330)	0.420005(540)
δ_K (kHz)	[b]	21.031(320)
Φ_J	[b]	[b]
Φ_{JK}	[b]	[b]
Φ_{KJ}	[b]	[b]
Φ_K	[b]	[b]
ϕ_K	[b]	[b]
ϕ_{JK}	[b]	[b]
ϕ_J	[b]	[b]
Interacting constants (in MHz): $C_A^1 = 47897.9(440)$, $C_A^2 = 2.756(370)$		

[a] When the Coriolis interaction is neglected (in MHz): $A = 56127.70(15)$, $B = 5898.587(51)$, $C = 5343.537(50)$.
[b] Fixed at the ground-state value [7].

$$^{CALC}C_A^1 = B_\alpha[(\omega_k/\omega_l)^{1/2} + (\omega_l/\omega_k)^{1/2}]\zeta_{kl}^a \quad (1)$$

the calculated value for the $CH_2{=}CH^{35}Cl$ species (respectively, for $CH_2{=}CH^{37}Cl$) with $\zeta_{kl}^a = -0.404$, $A = 57331.33$ MHz, $\omega_8 = 753.6\ cm^{-1}$, and $\omega_{12} = 647.7\ cm^{-1}$ (respectively, $A = 57247.45$ MHz, $\omega_8 = 747.7\ cm^{-1}$, and $\omega_{12} = 647.3\ cm^{-1}$) is $^{CALC}C_A^1 = 46422$ MHz (respectively, $^{CALC}C_A^1 = 46598$ MHz) to be compared with the experimental values (see Tables 4 and 5) $^{EXP}C_A^1 = 47857.0(400)$ MHz (respectively, $^{EXP}C_A^1 = 47897.9(440)$ MHz). The deviation is 3% or less.

Table 6
Statistical analysis of the results of the energy level calculations for the $\{12^1,8^1\}$ vibrational states of $CH_2{=}CH^{35}Cl$ and $CH_2{=}CH^{37}Cl$

	$CH_2{=}CH^{35}Cl$		$CH_2{=}CH^{37}Cl$	
Vibrational states:	12^1	8^1	12^1	8^1
Number of levels	1100	1321	475	1356
$0\times10^{-3} \leqslant \delta < 1\times10^{-3}\ cm^{-1}$ (%)	96.6	71.5	94.7	71.9
$1\times10^{-3} \leqslant \delta < 2\times10^{-3}\ cm^{-1}$ (%)	5.8	22.6	4.4	22.2
$2\times10^{-3} \leqslant \delta < 5\times10^{-3}\ cm^{-1}$ (%)	1.7	5.9	0.9	5.9
Standard deviation ($10^{-3}\ cm^{-1}$)	0.81		0.97	

3.4. Results and modelling of the experimental spectra

The results of the energy level calculations proved to be satisfactory for the $\{12^1,8^1\}$ resonating states. This good agreement can be seen from the infrared standard deviations and from the statistical analysis performed for the infrared energy levels (see Table 6).

In Figs. 1 and 2, we compare the observed and calculated spectra for different bands in various spectral regions. The synthetic spectra (line positions and relative intensities) were generated using the ground state constants taken from [7] and the upper state constants shown in Tables 4 and 5. It should be noted that only relative intensities were computed, since no attempts were made to derive experimental absolute intensities. Fig. 1 shows a detailed portion of the Q-branches of the ν_{12} bands of both isotopic species. Fig. 2 presents a portion of the P-branch near 577 cm^{-1}. The agreement is excellent between the observed and simulated spectra in both cases even for transitions with high K_a quantum numbers.

4. Ab initio structure

The structure has been calculated with the coupled cluster method with single and double excitations [23] augmented by a perturbational estimate of the connected triple excitations [CCSD(T)] [24]. The well-known Dunning's correlation consistent polarized valence basis sets, cc-pV(n+d)Z [25] where n = D, T, and Q, were employed. The frozen core approximation (fc) was used in these calculations. All calculations were performed with the MOLPRO2000 [26,27] program. The results are reported in Table 7. The coupled cluster T_1 diagnostic [28] which is 0.0105 at the CCSD(T)/cc-pV(Q+d)Z level indicates that non-dynamical electron correlation is not important and that the CCSD(T) results should be reliable. Improving the basis set from cc-pV(T+d)Z to cc-pV(Q+d)Z shows that convergence is definitely achieved for the C—H bond lengths (largest variation: −0.0008 Å for the C—H_{trans} bond length) and for the bond angles (largest variation 0.2° for the $\angle(CCH_g)$ angle). For the C=C and C—Cl bond lengths,

Table 7
Structure of vinyl chloride (bond lengths in Å, bond angles in degrees)

Method[a]	Basis	$C_1{=}C_2$	$C_1{-}Cl$	$C_1{-}H_g$[b]	$C_2{-}H_c$[b]	$C_2{-}H_t$[b]	∠(CCCl)	∠(CCH_g)	∠(CCH_c)	∠(CCH_t)
CCSD(T)	V(T+d)Z	1.3328	1.7345	1.0805	1.0814	1.0820	122.96	123.63	121.87	119.31
CCSD(T)	V(Q+d)Z	1.3297	1.7313	1.0799	1.0807	1.0812	122.80	123.86	121.83	119.27
MP2	V(Q+d)Z	1.3265	1.7207	1.0783	1.0781	1.0786	122.91	123.55	121.76	119.05
MP2	V(Q,5+d)Z	1.3260	1.7195	1.0788	1.0785	1.0790	122.85	123.59	121.74	119.04
CCSD(T)(ae)	MT	1.3254	1.7276	1.0779	1.0789	1.0793	123.05	123.52	121.92	119.33
CCSD(T)	MT	1.3283	1.7312	1.0793	1.0803	1.0807	123.01	123.57	121.92	119.31
MP2(ae)[c]	TZ2Pf	1.3260	1.7231	1.0752	1.0758	1.0764	123.17	123.25	121.97	119.05
Estimate *I*[d]		1.3263	1.7264	1.0785	1.0794	1.0798	122.78	123.82	121.83	119.29
Semi-experimental		1.3262(3)	1.7263(2)	1.0783(1)	1.0796(1)	1.0796(2)	122.75(1)	123.91(4)	121.77(2)	119.28(2)

[a] Unless noted otherwise: frozen core approximation; ae, all electrons correlated.
[b] *g*, geminal; *c*, *cis* to chlorine; *t*, *trans* to chlorine.
[c] The ab initio force field refers to this geometry.
[d] CCSD(T)/cc-pV(Q+d)Z + CCSD(T)(ae)/MT − CCSD(T)/MT for the C=C and C−Cl bonds, the correction MP2[cc-pV(Q,5+d)Z − cc-pV(Q+d)Z is also added, see text.

the variation is still −0.0031 Å indicating that these values might not have converged. To check this point, we have used a mixed basis set (cc-pV(5+d)Z on Cl, cc-pV5Z on C, and cc-pVQZ on H) at the MP2 level. The basis set enlargement has a non-negligible (but small) effect only for the C−Cl bond length which decreases by −0.0012 Å (and −0.0005 Å for C=C).

To estimate the core and core-valence correlation effects on the computed molecular geometry, the Martin–Taylor (MT) basis set[29] was used at the CCSD(T) level of theory. This correction leads to the expected shortening of the C=C (0.0029 Å) and C−H (0.0014 Å) bonds and to a much larger shortening of the C−Cl bond (0.0037 Å), whereas the angles are only slightly affected. It is known that the MP2 method with the correlation-consistent polarized weighted core-valence quadruple-ζ (cc-pwCVQZ) [30,31] is accurate for bond lengths between first row atoms [32] but overestimates the C−Cl bond correction by about 0.0013 Å [3]. This is indeed the case here, the MP2/cc-pwCVQZ method giving a core correction of 0.0055 Å for the C−Cl bond length but being in perfect agreement with the CCSD(T)/MT method for the other bond lengths. Adding all the CCSD(T)/MT core corrections to the CCSD(T)/cc-pV(Q,5+d)Z results, we arrive at the theoretical estimate for the equilibrium geometry, see Table 7.

5. Ab initio anharmonic force field

The ab initio force field was calculated at the MP2 level of theory using the Gaussian 03 program [33] with all electrons being correlated (ae approximation). The correlation-consistent polarized valence basis set TZ2Pf was used. It is a valence triple-ζ plus double polarization plus *f* function basis set consisting of Dunning's basis [34,35] supplemented with two sets of *d* and one set of *f* polarization functions [36]. The molecular geometry was first calculated. Then, the associated harmonic force field was evaluated analytically in Cartesian coordinates. The cubic (ϕ_{ijk}) and semi-diagonal quartic (ϕ_{ijkk}) normal coordinates force constants were determined with the use of a finite difference procedure involving displacements [37] along reduced normal coordinates (step size $\Delta q = 0.03$) and the calculation of analytic second derivatives at these displaced geometries. The evaluation of anharmonic spectroscopic constants was based on second-order rovibrational perturbation theory [38]. The anharmonic force field was calculated separately for all singly substituted isotopic species.

The harmonic wavenumbers ω_i, anharmonic corrections $\omega_i - \nu_i$, and vibrational band centers ν_i for $CH_2{=}CH^{35}Cl$ are given in Table 8. The agreement is rather good, the median of absolute deviations being only 17.2 cm^{-1} (1.35%). The same information is given in Table 9 for the isotopic species $CH_2{=}CH^{37}Cl$ and $CH_2{=}CD^{35}Cl$. It is interesting to note that the errors are mainly systematic and that the isotopic shifts are extremely well reproduced. For instance, the experimental isotopic shift for the CCl stretch is $\nu_8(^{35}Cl) - \nu_8(^{37}Cl) =$ 49.88 cm^{-1} whereas the ab initio value is 50.60 cm^{-1}.

The experimental ground state and computed equilibrium centrifugal distortion constants are compared in Table 10. The experimental data do not permit to determine the constants ϕ_{JK} and ϕ_K. For this reason, they were fixed at zero in the original work [7]. However, they are correlated with the other sextic constants (mainly Φ_{JK}), which makes a comparison with the ab initio constants meaningless. To circumvent this difficulty, we have repeated the fit of the rotational frequencies using the method of predicate observations [39], where some ab initio sextic constants are used as additional data with an appropriate uncertainty (10% of the value of the parameter) in the least-squares fit. For the quartic constants, the deviations between the experimental and ab initio values is only a few percent, the largest deviation (8.7%) being for δ_K, as usual. For the sextic constants, the overall agreement is also good with the

Table 8
Harmonic wavenumbers ω_i, anharmonic corrections $\omega_i - \nu_i$, and vibrational band centers ν_i for $CH_2{=}CH^{35}Cl$ (in cm^{-1})

Mode	Description	ω_i	$\omega_i - \nu_i$	ν_i(calc.)	ν_i(obs.)	o − c	Ref.
$\nu_1(a')$	CH stretch	3311.2	139.7	3171.5	3129	−42.5	[11]
$\nu_2(a')$	CH_2 antisym. stretch	3269.2	141.5	3127.7	3090	−37.7	[11]
$\nu_3(a')$	CH_2 sym. stretch	3211.9	129.3	3082.6	3040	−42.6	[11]
$\nu_4(a')$	C=C stretch	1665.5	39.3	1626.2	1614	−12.2	[11]
$\nu_5(a')$	CH_2 bend	1419.7	37.2	1382.5	1370.03	−12.4	[14]
$\nu_6(a')$	C=CH def.	1323.1	25.0	1298.1	1280.82	−17.2	[15]
$\nu_7(a')$	CH_2 rock	1053.6	15.6	1038.0	1030.91	−7.1	[17]
$\nu_8(a')$	CCl stretch	753.6	12.4	741.2	720.21	−20.3	This work
$\nu_9(a')$	C=CCl def.	401.7	1.0	400.7	395	−5.7	[11]
$\nu_{10}(a'')$	CH wag.	993.8	26.1	967.7	942.17	−25.5	[19]
$\nu_{11}(a'')$	CH_2 wag.	918.2	19.6	898.7	896.57	−2.1	[19]
$\nu_{12}(a'')$	Twist	647.7	10.6	637.1	618.57	−18.5	This work

Table 9
Harmonic wavenumbers ω_i, anharmonic corrections $\omega_i - \nu_i$, and vibrational band centers ν_i for $CH_2{=}CH^{37}Cl$ and $CH_2{=}CD^{35}Cl$ (in cm^{-1})

Mode	Description	ω_i	$\omega_i - \nu_i$	ν_i(calc.)	ν_i(obs.)	o − c
	$CH_2{=}CH^{37}Cl$					
$\nu_1(a')$	CH stretch	3311.2	139.7	3171.5	3120.4[a]	−51.1
$\nu_2(a')$	CH_2 antisym. stretch	3269.2	141.6	3127.7	3086.0[a]	−41.7
$\nu_3(a')$	CH_2 sym. stretch	3211.9	129.3	3082.6	3034.2[a]	−48.4
$\nu_4(a')$	C=C stretch	1665.4	39.4	1626.0	1612.6[a]	−13.4
$\nu_5(a')$	CH_2 bend	1419.7	37.4	1382.2	1369.71[a]	−12.5
$\nu_6(a')$	C=CH def.	1323.0	25.0	1297.9	1280.74[a]	−17.2
$\nu_7(a')$	CH_2 rock	1053.0	15.6	1037.4	1030.45[a]	−7.0
$\nu_8(a')$	CCl stretch	747.7	12.2	735.5	715.41[c]	−20.1
$\nu_9(a')$	C=CCl def.	399.4	1.0	398.4	393[a]	−5.4
$\nu_{10}(a'')$	CH wag.	993.8	26.1	967.7	942.1[a]	−25.6
$\nu_{11}(a'')$	CH_2 wag.	918.2	19.6	898.7	896.5[a]	−2.2
$\nu_{12}(a'')$	Twist	647.3	10.6	636.8	618.2[c]	−18.6
	$CH_2{=}CD^{35}Cl$					
$\nu_1(a')$	CH stretch	3310.2	139.3	3170.9	3125[b]	−45.9
$\nu_2(a')$	CH_2 antisym. stretch	3213.3	139.5	3073.8	3045[b]	−28.8
$\nu_3(a')$	CD stretch	2419.2	78.3	2340.9	2305[b]	−35.9
$\nu_4(a')$	C=C stretch	1648.3	39.0	1609.3	1598[b]	−11.3
$\nu_5(a')$	CH_2 bend	1412.8	40.4	1372.4	1364[b]	−8.4
$\nu_6(a')$	CH_2 rock	1137.3	22.4	1114.9	1120[b]	5.1
$\nu_7(a')$	C=CD def.	887.5	11.2	876.3		
$\nu_8(a')$	CCl stretch	744.2	11.8	732.4	706[b]	−26.4
$\nu_9(a')$	C=CCl def.	398.2	1.0	397.3		
$\nu_{10}(a')$	CH_2 wag.	922.8	20.8	902.0	904[b]	2.0
$\nu_{11}(a'')$	CD wag.	842.4	19.0	823.4	808[b]	−15.4
$\nu_{12}(a'')$	CH wag.	615.5	9.7	605.7	588[b]	−17.7

[a] Ref. [14].
[b] Ref. [11].
[c] This work.

exception of Φ_{JK} which shows a deviation of 30.8%. However, this parameter is not as well determined as its standard deviation seems to indicate. Actually, its value is quite sensitive to the values of the predicate observations φ_{JK} and φ_K (note that Φ_{JK} becomes negative when φ_{JK} and φ_K are fixed at zero).

The experimental and ab initio rotation–vibration interaction constants (α-constants) are compared in Table 11. The agreement is rather good taking into account the fact that many states are in interaction. Particularly, it has to be noted that the large variations of the A rotational constant are well reproduced by the ab initio force field.

6. Semi-experimental equilibrium structure

The theoretical rotation–vibration interaction constants deduced from the ab initio force field were combined with the known experimental ground state

Table 10
Experimental and ab initio quartic (kHz) and sextic (Hz) centrifugal distortion constants for CH_2=$CH^{35}Cl$

	Obs.	Calc.	o − c	(o−c)%
Δ_J	3.07082(29)	2.9518	0.1190	3.9
Δ_{JK}	−42.2463(38)	−44.251	2.005	−4.7
Δ_K	1290.54(39)	1321.3	−30.8	−2.4
δ_J	0.44929(12)	0.4300	0.0193	4.3
δ_K	18.782(22)	17.15	1.63	8.7
Φ_J	0.002475(51)	0.00205	0.00042	16.9
Φ_{JK}	0.0328(14)	0.02270	0.01012	30.8
Φ_{KJ}	−5.1647(79)	−4.8237	−0.3410	6.6
Φ_K	108.3(91)	99	9	8.0
ϕ_J	0.000936(32)	0.001020	−0.00008	−9.0
ϕ_{JK}[a]	0.034999(38)	0.035042		
ϕ_K[a]	7.758(95)	7.810		

[a] Predicate observation, see text.

rotational constants [6] to yield the semi-experimental equilibrium rotational constants of Table 12. We have only used the constants of [6] because mixing sets of rotational constants is a questionable practice: a small incompatibility of the sets would affect the accuracy of the structure determination whereas the error practically compensates if all lines are measured and analyzed in the same way. The equilibrium inertial defect is also given in this table. It is about two orders of magnitude smaller than the ground state inertial defect, indicating that the equilibrium rotational constants are rather accurate. However, it is not exactly zero as it should be. This is probably mainly due to the limited accuracy of the computed rotation–vibration interaction constants. The equilibrium structure was calculated from a weighted least-squares fit of the semi-experimental moments of inertia and is given in Table 7. It is in excellent agreement with the ab initio structure of the previous section. Assuming the errors of the respective rotational constants (Table 12) proportional to 5:1:1, a standard deviation of the fit $\sigma = 1$ is obtained for the error estimates (in MHz) $\sigma(A_e) = 0.32$, $\sigma(B_e) = 0.06$, and $\sigma(C_e) = 0.06$.

Table 11
Experimental and ab initio rotation–vibration interaction constants (MHz) for vinyl chloride

Mode i	α_i^A		α_i^B		α_i^C		Ref.
	Obs.	Calc.	Obs.	Calc.	Obs.	Calc.	
^{35}Cl							
5	−263.7	−222.1	0.3	−1.7	6.1	3.9	[14]
6	411.1	203.9	−10.5	−13.4	0.3	−0.1	[15]
7	−734.6	−782.0	−19.0	−28.5	8.5	8.2	[17]
8	−644.9	−662.2	30.7	28.1	25.7	23.6	[18][a]
9		−180.3	2.6	0.5	7.5	6.2	This work
10	484.5	563.5	21.6	29.9	−3.2	−2.9	[19]
11	777.8	779.8	8.3	6.5	−0.6	−1.6	[19]
12	578.0	580.9	5.2	4.8	−2.5	−2.3	This work[a,b]
^{37}Cl							
5	−276.5	−222.1	0.9	−1.6	6.4	3.8	[14]
6	449.0	203.2	−10.0	−12.9	0.2	−0.2	[16]
7	−730.8	−789.2	−18.2	−27.7	8.1	7.9	[17]
8	−694.8	−712.8	29.9	27.4	25.2	23.1	[18][a]
12	629.2	633.6	5.0	4.6	−2.3	−2.2	This work[a,b]

[a] Coriolis interaction neglected.
[b] Constants given at the bottom of Tables 4 and 5.

Table 12
Semi-experimental equilibrium rotational constants (MHz) for vinyl chloride

	A_e		B_e		C_e		Δ_e[a]	Δ_0[b]
	Obs.	o − c	Obs.	o − c	Obs.	o − c		
H_2C=$CH^{35}Cl$	57331.33	−0.04	6056.02	−0.06	5477.49	0.01	−0.0010	0.1074
H_2C=$CH^{37}Cl$	57247.45	−0.26	5929.00	−0.04	5372.61	0.00	−0.0007	0.1079
$H_2{}^{13}C$=$CH^{35}Cl$	56795.77	0.23	5851.87	0.02	5305.29	0.05	−0.0006	0.1082
H_2C=$^{13}CH^{35}Cl$	55734.38	0.15	6024.82	−0.00	5437.13	0.05	−0.0008	0.1103
HDC=$CH^{35}Cl$[c]	57226.34	−0.02	5571.55	−0.02	5077.27	0.03	−0.0008	0.1026
HDC=$CH^{35}Cl$[d]	47627.14	0.03	5870.38	−0.01	5226.24	0.02	−0.0005	0.1172
H_2C=$CD^{35}Cl$	44799.30	0.01	6017.30	−0.04	5304.85	0.04	−0.0013	0.1175

[a] Equilibrium inertial defect (in u Å^2).
[b] Ground state inertial defect (in u Å^2).
[c] D in *trans* position.
[d] D in *cis* position.

These values are roughly compatible with the columns o − c of Table 12.

7. Experimental structures

The experimental ground state rotational constants of 20 isotopologs given in [6] were used as input to a program for iterated, weighted and correlated linear least-squares-fitting the experimental 3×20 inertial moments to yield the nine independent structural parameters of the planar molecule plus up to six optional ro-vibrational parameters The more recent models for the mass-dependent rotation–vibration interaction contributions to the inertial moments [2] can be applied: $r_m^{(1)}$, and $r_m^{(2)}$, as well as $r_m^{(1L)}$ and $r_m^{(2L)}$ (the latter two including a "Laurie-correction" for $H \rightarrow D$ substitution). The program uses true derivatives, recalculated in each iteration cycle, instead of difference quotients for all elements of the least-squares coefficient matrix (or design matrix) ∂(inertial moment)/∂(parameter). This obviates the necessity for choosing adequate step widths and allows the iterations to continue until the parameter changes from cycle to cycle are no larger than the truncation errors of the arithmetic used.

It is often argued that in cases where the residuals of the rotational constants (or inertial moments) after the fit prove to be much larger than their experimental errors, these errors have lost their credibility (most often due to shortcomings of the model) and that unity-weighting is to be preferred over a weighting depending on the experimental errors. However, this neglects the fact that the proportions of the errors of the rotational constants, err(A):err(B):err(C), are primarily due to the transition types of the lines that could be measured and their respective numbers, which are usually very similar for all isotopologs included in the set. The errors of the constants A, B, and C therefore have an inherently different influence on the result of the fit which should be retained even if their errors are large. Therefore, we have used for all experimental models listed in Table 13 the uncorrelated average errors (in MHz), $\overline{\text{err}}(A) = 0.05080$, $\overline{\text{err}}(B) = 0.01985$, and $\overline{\text{err}}(C) = 0.00615$ (which are evidently very different) as the basis for computing the weights of the inertial moments of *all* isotopologs. In the present case, the (dimensionless) standard deviation of the fit σ reflects the factor by which the errors $\overline{\text{err}}$ have been effectively increased by imperfections of the model before the program computes the standard errors of the parameters.

Table 13 displays the results of all fits made in terms of bonding and rovib parameters, while Table 14 shows the atomic coordinates in the principal inertial axis system of the parent molecule $H_2C{=}CH^{35}Cl$. For all models calculated, two rows have been included in Table 13

Table 13
Vinyl chloride: different least-squares-fits of experimental rotational constants to obtain structure and rovib data (lengths in Å, angles in degrees, rovib-C in u$^{1/2}$ Å, rovib-D in u$^{1/2}$ Å^2, μ in u$^{-1/2}$, δ_H in u$^{1/2}$ Å)

	r_0	$r_m^{(1)}$	$r_m^{(2)}$ mod[a]	$r_m^{(1L)}$[b]	r_s-fit	r_s-fit + com[c]	Semi-experimental[f]	r_e[f]
Std. dev. fit σ[d]	220.2	30.52	27.99	29.38	12.93	12.55	0.0658	
$r(C_1{=}C_2)$	1.3298(63)	1.3270(10)	1.3272(9)	1.3285(11)	1.3312(28)	1.3288(15)	1.3262(3)	1.3263
$r(C_1{-}Cl)$	1.7336(53)	1.7253(12)	1.7268(15)	1.7263(13)	1.7278(12)	1.7283(6)	1.7263(2)	1.7264
$r(C_1{-}H_g)$[g]	1.0782(09)	1.0782(1)	1.0779(3)	1.0752(14)	1.0805(16)	1.0815(12)	1.0783(1)	1.0785
$r(C_2{-}H_c)$[g]	1.0837(16)	1.0832(2)	1.0834(3)	1.0807(12)	1.0873(31)	1.0887(10)	1.0796(1)	1.0794
$r(C_2{-}H_t)$[g]	1.0825(41)	1.0800(7)	1.0787(10)	1.0757(21)	1.0779(24)	1.0767(17)	1.0796(2)	1.0798
(C_2,C_1,Cl)	122.57(15)	122.81(4)	122.84(4)	122.76(5)	122.72(20)	122.86(11)	122.75(1)	122.78
$\angle(C_2,C_1,H_g)$[g]	123.65(72)	123.11(12)	123.30(20)	123.34(16)	123.22(14)	123.21(8)	123.91(4)	123.82
$\angle(C_1,C_2,H_c)$[g]	121.26(45)	121.14(7)	121.01(10)	121.09(7)	121.05(14)	120.98(7)	121.77(2)	121.83
$\angle(C_1,C_2,H_t)$[g]	118.80(30)	119.29(7)	119.28(10)	119.24(7)	119.67(38)	119.84(26)	119.28(2)	119.29
r.m.s. diff(r)[e]	0.0042	0.0018	0.0019	0.0016	0.0044	0.0048	0.0002	
r.m.s. diff($\angle$)[e]	0.40	0.50	0.49	0.44	0.53	0.59	0.06	
δ_H				0.0109(50)				
Rovib-$C(a)$		0.027(3)	0.028(03)	0.004(11)				
Rovib-$C(b)$		0.040(9)	0.029(15)	0.028(11)				
Rovib-$C(c)$		0.058(9)	0.033(15)	0.039(12)				
Rovib-$D(c)$			0.087(52)					

[a] In this fit two rovib parameters were constrained with assumed errors: rovib-$D(a) = 0.000(4)$, rovib-$D(b) = 0.00(5)$, the errors in this column include the errors of the parameters constrained.

[b] All C—H bond lengths in this column are r_m values in $r_{eff} = r_m + \mu \cdot \delta_H$, see [2].

[c] Com: 3 center of mass conditions imposed (two first-order equations for principal inertial axes a and b, one second-order equation for (a b)).

[d] The average errors of the experimental rotational constants were used for *all* isotopologs in the weighted lsq-fits, see text.

[e] Root-mean-square differences of data of current column with respect to ab initio data of last column, separately for lengths and angles, for column $r_m^{(1L)}$ the three C—H bond lengths are r_m values [b] which have not been not included in r.m.s. diff(r).

[f] See Table 7 and text, Section 6.

[g] g, geminal; c, *cis* to chlorine; t, *trans* to chlorine.

Table 14
Vinyl chloride, atomic coordinates in the principal inertial axis system of the parent, as computed from the bond variables of Table 13

Atom	r_0	$r_m^{(1)}$	$r_m^{(2)}$ mod	$r_m^{(1L)}$[b]	r_s-fit	r_s-fit + com[c]	Semi-experimental	r_e (I)[d]
C_1								
a	−0.6651(48)	−0.6604(9)	−0.6614(13)	−0.6606(8)	−0.6602(13)	−0.6616(5)	−0.6611(2)	−0.6611
b	0.5098(4)	0.5067(3)	0.5067(5)	0.5076(5)	0.5088(17)	0.5076(12)	0.5073(0)	0.5071
H_g[a]								
a	−0.7368(77)	−0.7380(14)	−0.7351(33)	−0.7348(20)	−0.7360(8)	−0.7363(7)	−0.7244(5)	−0.7256
b	1.5857(8)	1.5822(4)	1.5820(5)	1.5912(41)	1.5866(4)	1.5865(3)	1.5837(0)	1.5836
Cl								
a	0.9643(6)	0.9613(5)	0.9619(8)	0.9618(6)	0.9629(2)	0.9629(2)	0.9613(0)	0.9615
b	−0.0823(4)	−0.0821(1)	−0.0821(1)	−0.0823(1)	−0.0832(28)	−0.0824(2)	−0.0826(0)	−0.0825
C_2								
a	−1.7206(29)	−1.7169(9)	−1.7182(14)	−1.7180(10)	−1.7199(5)	−1.7203(3)	−1.7165(1)	−1.7168
b	−0.2990(7)	−0.2962(2)	−0.2961(3)	−0.2967(4)	−0.2968(31)	−0.2954(9)	−0.2958(0)	−0.2957
H_c[a]								
a	−1.6036(37)	−1.6020(9)	−1.6010(16)	−1.6007(11)	−1.6026(4)	−1.6027(3)	−1.6130(3)	−1.6149
b	−1.3763(16)	−1.3733(3)	−1.3732(5)	−1.3821(41)	−1.3778(4)	−1.3777(4)	−1.3704(1)	−1.3703
H_t[a]								
a	−2.7115(22)	−2.7074(7)	−2.7074(10)	−2.7145(33)	−2.7115(2)	−2.7116(2)	−2.7069(2)	−2.7074
b	0.1368(45)	0.1341(7)	0.1340(17)	0.1368(13)	0.1258(40)	0.1250(39)	0.1339(2)	0.1342

[a] *g*, geminal; *c*, *cis* to chlorine; *t*, *trans* to chlorine.
[b] For $r_m^{(1L)}$ the hydrogen coordinates correspond to the bond lengths r_{eff}(H) of Table 15.
[c] Com: 3 center of mass conditions imposed (two first-order equations for principal inertial axes *a* and *b*, one second-order equation for (*a*,*b*)).
[d] Estimate *I*, see Table 7.

which show the r.m.s. differences, separately for bond lengths and angles, between the structure parameters of the current model and the ab initio estimate I of Table 7 which has been added as a last column to Table 13 for convenience.

Comparing σ of the r_0 (effective structure) and the $r_m^{(1)}$ model, the great progress made by the introduction of the mass-dependent rovib model [2] is documented. Comparison of the respective r.m.s. differences further shows that the $r_m^{(1)}$ model has also come a good deal nearer to the ab initio estimate.

An attempt to apply the complete $r_m^{(2)}$ model hardly brought about an improvement over $r_m^{(1)}$, the additional rovib parameters were highly correlated and the rovib parameters $D(a)$ and $D(b)$ were effectively zero-valued. For the modified model $r_m^{(2)}$ mod listed in Table 13, $D(a)$ and $D(b)$ have been constrained to zero with large enough (uncorrelated) errors.

The $r_m^{(1L)}$ model [2] in Table 13 combines the $r_m^{(1)}$ model with a correction to take care of the bond length shortening upon H → D substitution, known as "Laurie correction," by expressing the hydrogen bond length at a particular hydrogen position as $r_{eff}(H) = r_m + \mu(H) \cdot \delta_H$ and $r_{eff}(D) = r_m + \mu(D) \cdot \delta_H$, respectively, with known mass-dependent factors $\mu(H)$ and $\mu(D)$ and adjustable r_m and δ_H. Structurally different hydrogen positions would require different pairs of r_m and δ_H for each hydrogen position. Earlier experience (with larger molecules) had shown us that it is rarely possible to fit independently both parameters, r_m as well as δ_H, even if there is no more than one hydrogen position or one set of structurally equivalent hydrogen positions in the molecule. While it was indeed impossible to fit three independent sets of the two quantities r_m and δ_H for the three different hydrogen positions in vinyl chloride owing to extremely high correlations and convergence to irrational results, a fit which permitted three different lengths r_m but required one *common* δ_H was successful and produced $\delta_H = 0.0109(50)$ u$^{1/2}$ Å, a certainly acceptable value, though with a large error. The value of δ_H is very near of 0.010 u$^{1/2}$ Å, which is expected in [2] and yields a Laurie correction of 0.0028 Å, again very near the value 0.003 Å expected for this correction (within rather wide limits). Neither the effective C—H bond lengths r_{eff}(H) nor the lengths r_m for the three different hydrogen positions in vinyl chloride can be directly compared with the respective equilibrium bond lengths r_e of the ab initio estimate in Table 13, the hydrogen positions have therefore been skipped when computing the r.m.s. differences for column $r_m^{(1L)}$. We have collected the values r_{eff}(H) and r_{eff}(D) for the three structurally different hydrogen positions in Table 15.

The results of the r_s-fit method [40] are also displayed in Tables 13 and 14. The standard deviations sigma of the r_s-fits cannot be compared with the values of sigma of the r_0- and r_m-fits owing to the very different statement of the least-squares-problem for the r_s-fit method. As anticipated, the results of the r_s-fit deserve no preference over the r_m methods which is confirmed by an inspection of the r.m.s. differences.

Table 15
Vinyl chloride: least-squares-fit $r_m^{(1L)}$ (H: r_m): values obtained for r_m, $r_{eff}(H)$, $r_{eff}(D)$ in equation $r_{eff} = r_m + \mu \cdot \delta_H$ for H or D in the respective hydrogen positions[a]

Lengths (in Å)	Hydrogen positions[b]		
	g	*c*	*t*
r_m[a]	1.0752(14)	1.0807(12)	1.0757(21)
δ_H		0.0109(50)	
$r_{eff}(H)$	1.0862(37)	1.0917(24)	1.0867(31)
$r_{eff}(D)$	1.0830(22)	1.0886(39)	1.0835(18)
Difference H − D	0.0032	0.0032	0.0032

[a] The r_m are three *separate* parameters for positions *g*, *c*, *t*. While δ_H had to be chosen as a *common* parameter for all three positions. Within the number of digits displayed, $r_{eff}(H)$ and $r_{eff}(D)$ are independent of H or D being present in neighboring hydrogen positions.
[b] *g*, geminal; *c*, *cis* to chlorine; *t*, *trans* to chlorine.

Table 14 makes evident a vexing and yet unexplained feature: the coordinate $a(H_{cis})$ is in *all* experimental determinations up to 0.015 Å larger than this coordinate is in the the ab initio estimate (and in the semi-experimental result), this difference is much larger than the corresponding differences for all other coordinates. This large value appears to be out of place. Both, $a(H_{cis})$ and $b(H_{cis})$ are large coordinates, the small-coordinate argument for lacking accuracy is therefore not applicable. If this coordinate were left out of the r.m.s. length difference computed for, e.g., $r_m^{(1)}$, this value would drop down from 0.0018 to 0.0005 Å. The discrepancy mentioned for the coordinate a(cH) is transferred to the bond parameters of H_{cis} in Table 13. Nonetheless, the agreement of the experimental $r_m^{(1)}$ determination with the ab initio estimate *I* can be considered as good to excellent, the statement could probably be extended to the $r_m^{(1L)}$ structure if a reliable reference between r_m and r_{eff} on the one hand and r_e on the other could be established.

8. Discussion

The anharmonic force field of vinyl chloride has been calculated at the MP2/TZ2Pf level of theory. Comparison of experimental and calculated spectroscopic parameters shows that this force field is accurate. The ab initio force field was also used to determine a semi-experimental equilibrium structure which was found to be in excellent agreement with the CCSD(T) ab initio structure. The experimental r_m mass-dependent structures have also been calculated and, for the heavy atom skeleton, they are found to be in excellent agreement with both, the experimental and the ab initio structure. For the CH bonds, the agreement is worse. The ab initio and semi-experimental structures give $r(CH_t) > r(CH_c) > r(CH_g)$ whereas the r_m structures give: $r(CH_c) > r(CH_t) > r(CH_g)$. Generally, for the CH bonds, ab initio results are more reliable than experimental values [1]. Furthermore, in the particular case of vinyl chloride, McKean [12] was able to determine the isolated stretching frequencies of the three CH bonds which are (in cm^{-1}): $\nu(CH_t) = 3072 < \nu(CH_c) = 3074 < \nu(CH_g) = 3082$, the accuracy being about $\pm 3\ cm^1$. These values give (in Å): $r(CH_t) = 1.0805 > r(CH_c)$ 1.0803 $> r(CH_g)$ 1.0798 [41]. They are in excellent agreement with the ab initio results.

To estimate the accuracy, the range of the data was used [42]. For the CC and CCl bonds, the ab initio, semi-experimental, as well as the $r_m^{(1)}$, $r_m^{(2)}$, and $r_m^{(1L)}$ structures were used. It allows us to establish that a realistic estimate of the standard deviations is: $\sigma[r(C{=}C)] = 0.0010$ Å, $\sigma[r(C{-}Cl)] = 0.0006$ Å, and $\sigma[\angle(CCCl)] = 0.038°$. This method cannot be used for the CH bonds because the r_m structures are not reliable enough for these bonds. However, the extremely good agreement between the r(CH) bond lengths derived from the isolated stretching frequencies, the ab initio and the semi-experimental structures, indicates that the r(CH) bond lengths are also quite precise. The conclusion is that the derived structure seems to be extremely precise with an accuracy probably as good as 0.001 Å for the bond lengths and 0.1° for the bond angles. The ab initio and semi-experimental structures are almost identical for all parameters. Thus, as the preferred structure, we suggest the mean value of these two structures.

Acknowledgments

We are indebted to the Laboratoire Européen de Spectroscopie Moléculaire for financial support. H.D.R. thanks the Fonds der Chemischen Industrie, Frankfurt/Main, for support. The authors thank A. De Lorenzi and S. Gorgianni for sending the list of assigned transitions in the ν_8 bands of the two main $CH_2{=}CHCl$ isotopologs.

References

[1] J. Demaison, G. Wlodarczak, H.D. Rudolph, in: M. Hargittai, I. Hargittai (Eds.), Advances in Molecular Structure Research, vol. 3, JAI Press, Greenwich, CT, 1997, pp. 1–51.
[2] J.K.G. Watson, A. Roytburg, W. Ulrich, J. Mol. Spectrosc. 196 (1999) 102–129.
[3] J. Demaison, J.E. Boggs, H.D. Rudolph, J. Mol. Struct. 695-696 (2004) 145–153, and references therein.
[4] R.C. Ivey, M.I. Davis, J. Chem. Phys. 57 (1972) 1909–1911.
[5] D. Kivelson, E.B. Wilson, D.R. Lide, J. Chem. Phys. 32 (1960) 205–209.
[6] M. Hayashi, T. Inagusa, J. Mol. Struct. 220 (1990) 103–117.
[7] I. Merke, L. Poteau, G. Wlodarczak, A. Bouddou, J. Demaison, J. Mol. Spectrosc. 177 (1996) 232–239.
[8] D. Coffey, B.J. Smith, L. Radom, J. Chem. Phys. 98 (1993) 3952–3959.
[9] C. Møller, M.S. Plesset, Phys. Rev. 46 (1934) 618–622.

[10] C.W. Gullikson, R.J. Nielsen, J. Mol. Spectrosc. 1 (1957) 158–178.
[11] S. Enomoto, M. Asashina, J. Mol. Spectrosc. 19 (1966) 117–130.
[12] D.C. McKean, Spectrochim. Acta A 31 (1975) 1167–1186.
[13] R. Elst, A. Oskam, J. Mol. Spectrosc. 40 (1971) 84–94.
[14] S. Giorgianni, P. Stoppa, A. De Lorenzi, Mol. Phys. 92 (1997) 301–306.
[15] S. Giorgianni, A. De Lorenzi, M. Pedrali, P. Stoppa, S. Ghersetti, J. Mol. Spectrosc. 156 (1992) 373–382.
[16] S. Giorgianni, A. De Lorenzi, P. Stoppa, A. Baldan, S. Ghersetti, J. Mol. Spectrosc. 164 (1994) 550–558.
[17] P. Stoppa, S. Giorgianni, S. Ghersetti, Mol. Phys. 91 (1997) 215–222.
[18] A. De Lorenzi, S. Giorgianni, R. Bini, Mol. Phys. 96 (1999) 101–108.
[19] A. De Lorenzi, S. Giorgianni, R. Bini, Mol. Phys. 98 (2000) 355–362.
[20] G.A. Guirgis, K.-M. Marstokk, H. Møllendal, Acta Chem. Scand. 45 (1991) 482–490.
[21] M.C.L. Gerry, Can. J. Chem. 49 (1971) 255–264.
[22] R.A. Toth, J. Opt. Soc. Am. B 8 (1991) 2236–2255.
[23] G.D. Purvis III III, R.J. Bartlett, J. Chem. Phys. 76 (1982) 1910–1918.
[24] K. Raghavachari, G.W. Trucks, J.A. Pople, M. Head-Gordon, Chem. Phys. Lett. 157 (1989) 479–483.
[25] T.H. Dunning Jr., K.A. Peterson, A.K. Wilson, J. Chem. Phys. 114 (2001) 9244–9253.
[26] MOLPRO 2000 is a package of ab initio programs written by H.-J. Werner and P.J. Knowles, with contributions from R.D. Amos, A. Bernhardsson, A. Berning, P. Celani, D.L. Cooper, M.J.O. Deegan, A.J. Dobbyn, F. Eckert, C. Hampel, G. Hetzer, T. Korona, R. Lindh, A.W. Lloyd, S.J. McNicholas, F.R. Manby, W. Meyer, M.E. Mura, A. Nicklass, P. Palmieri, R. Pitzer, G. Rauhut, M. Schütz, H. Stoll, A.J. Stone, R. Tarroni, T. Thorsteinsson.
[27] P.J. Knowles, C. Hampel, H.-J. Werner, J. Chem. Phys. 112 (2000) 3106–3107.
[28] T.J. Lee, P.R. Taylor, Int. J. Quantum Chem. Symp. 23 (1989) 199–207.
[29] J.M.L. Martin, P.R. Taylor, Chem. Phys. Lett. 225 (1994) 473–479.
[30] D.E. Woon, T.H. Dunning Jr., J. Chem. Phys. 103 (1995) 4572–4585.
[31] K.A. Peterson, T.H. Dunning Jr., J. Chem. Phys. 117 (2002) 10548–10560.
[32] L. Margulès, J. Demaison, H.D. Rudolph, J. Mol. Struct. 599 (2001) 23–30.
[33] M.J. Frisch, G.W. Trucks, H.B. Schlegel, G.E. Scuseria, M.A. Robb, J.R. Cheeseman, J.A. Montgomery Jr., T. Vreven, K.N. Kudin, J.C. Burant, J.M. Millam, S.S. Iyengar, J. Tomasi, V. Barone, B. Mennucci, M. Cossi, G. Scalmani, N. Rega, G.A. Petersson, H. Nakatsuji, M. Hada, M. Ehara, K. Toyota, R. Fukuda, J. Hasegawa, M. Ishida, T. Nakajima, Y. Honda, O. Kitao, H. Nakai, M. Klene, X. Li, J.E. Knox, H.P. Hratchian, J.B. Cross, C. Adamo, J. Jaramillo, R. Gomperts, R.E. Stratmann, O. Yazyev, A.J. Austin, R. Cammi, C. Pomelli, J.W. Ochterski, P.Y. Ayala, K. Morokuma, G.A. Voth, P. Salvador, J.J. Dannenberg, V.G. Zakrzewski, S. Dapprich, A.D. Daniels, M.C. Strain, O. Farkas, D.K. Malick, A.D. Rabuck, K. Raghavachari, J.B. Foresman, J.V. Ortiz, Q. Cui, A.G. Baboul, S. Clifford, J. Cioslowski, B.B. Stefanov, G. Liu, A. Liashenko, P. Piskorz, I. Komaromi, R.L. Martin, D.J. Fox, T. Keith, M.A. Al-Laham, C.Y. Peng, A. Nanayakkara, M. Challacombe, P.M.W. Gill, B. Johnson, W. Chen, M.W. Wong, C. Gonzalez, J.A. Pople, Gaussian, Inc., Pittsburgh PA, 2003, Revision B.04.
[34] T.H. Dunning Jr., J. Chem. Phys. 55 (1971) 716–723.
[35] A.D. McLean, G.S. Chandler, J. Chem. Phys. 72 (1980) 5639–5648.
[36] T.H. Dunning Jr., J. Chem. Phys. 90 (1989) 1007–1023.
[37] W. Schneider, W. Thiel, Chem. Phys. Lett. 157 (1989) 367–373.
[38] D. Papousek, M.R. Aliev, Molecular Vibrational-rotational Spectra, Elsevier, Amsterdam, 1982.
[39] L.S. Bartell, D.J. Romanesko, T.C. Wong, in: G.A. Sims, L.E. Sutton (Eds.), Chemical Society Specialist Periodical Report No. 20: Molecular Structure by Diffraction Methods, vol. 3, The Chemical Society London, 1975, p. 72.
[40] V. Typke, J. Mol. Spectrosc. 69 (1978) 173–178.
[41] J. Demaison, G. Wlodarczak, Struct. Chem. 5 (1994) 57–66.
[42] G.C. Kyker, Am. J. Phys. 51 (1983) 852.